J Mater Sci (2011) 46:7770–7775
DOI 10.1007/s10853-011-5756-5

Controllable white light emission from Dy^{3+}–Eu^{3+} co-doped $KCaBO_3$ phosphor

Subrata Das · A. Amarnath Reddy · S. Surendra Babu · G. Vijaya Prakash

Received: 31 March 2011 / Accepted: 28 June 2011 / Published online: 20 July 2011

Abstract Potassium calcium borate, $KCaBO_3$:Eu^{3+} phosphors with various Dy^{3+} concentrations (0–3 wt%) were synthesized by solid state reaction and studied for the first time. Under various UV–violet excitations, the obtained single monoclinic phased Dy^{3+}–Eu^{3+} co-doped $KCaBO_3$ polycrystalline phosphors emit a combination of yellow–blue and red–orange wavelength giving intense white light, which can easily be controlled by varying the concentration of Dy^{3+}. The increase in white light emission with the increase of Dy^{3+} concentration indicates the efficient energy inter-ion transfer from Dy^{3+} to Eu^{3+} ions. Furthermore, the observed emission lifetimes and the intense white light emission are suggestive exploration for the present phosphor for potential optoelectronic applications such as white light-emitting phosphor for blue LEDs chips.

Introduction

Stable and highly emissive white light-emitting phosphors are important for display and lighting technologies. The majority of commercially available lamp phosphors require excitation by near ultraviolet (NUV) light for operation, a requirement that has led to the almost universal use of a mercury vapor plasma in fluorescent lighting products [1]. The development of new materials that convert NUV light light into visible light could help replace the mercury currently used in fluorescent lights with a less toxic alternative and lead to higher net conversion efficiencies [1–3]. In addition, the emissive centers used in fluorescent lamp or cathodoluminescent display phosphors are typically expensive or environmentally toxic metals such as silver, cadmium, germanium, or rare earth elements [1–3]. Up to now, a few white light-emitting phosphors suitable for NUV excitation have been reported [4–7], the phosphors with better optical properties are still in development. Moreover, many of these phosphors suffer from issues like low efficiency, toxic, and unstable. In addition, white LEDs are generally fabricated by using two or three different kinds of phosphors and re-absorption of emission wavelengths leads to a decrease in luminous efficiency [8, 9]. Therefore, it is essential to exploit single-phased full-color-emitting phosphors for NUV-pumped white LED [8, 9]. In the past few years, many types of single-phased borates are extensively studied and used as efficient optoelectronic materials because they show excellent colorimetric purity, good luminescence characteristics under NUV excitation, and high chemical stability [10–14]. Borates like BaB_2O_4 [15], LiB_3O_5 [16], $CsLiB_6O_{10}$ [17], $K_2Al_2B_2O_7$ [18] possess high non-linear optical (NLO) properties. Specially rare earth doped crystalline borates such as $Ca_4GdO(BO_3)_3$ [19], $YAl_3(BO_3)_4$ [20], and $Li_2B_4O_7$ [21] have proven to be among the preferred choice for solid state laser materials and plasma display panels (PDP). $Li_2B_4O_7$ single crystal [22], MgB_4O_7:Dy,Na [23], and $Sr_2B_5O_9Cl$:Eu [24] phosphors are used in commercial dosimetry systems. Eu-doped alkaline haloborates are considered for the neutron radiography [25–27] using photo stimulated luminescence

---

S. Das (✉) · A. Amarnath Reddy · G. Vijaya Prakash (✉)
Nanophotonics Laboratory, Department of Physics, Indian Institute of Technology Delhi, New Delhi 110016, India
e-mail: phy_subrata@yahoo.co.in

G. Vijaya Prakash
e-mail: prakash@physics.iitd.ac.in

S. Surendra Babu
Laser Instrumentation Design Centre, Instrument Research and Development Establishment, Dehradun 248008, India

(PSL). Pr^{3+} doped borate materials exhibit interesting cascade emission [28]. $(Ce_{0.3}Gd_{0.5}Tb_{0.2})MgB_5O_{10}$ is a green emitting phosphor used in the tri-color lamps [29]. Also $(Gd_{0.6}Ce_{0.2}–Tb_{0.2})Mg_{0.9}Mn_{0.1}B_5O_{10}$ phosphor is used in deluxe lamps with high color rendition index [30]. $SrB_4O_7:Eu^{2+}$ phosphor is used in commercial sun-tanning lamps [31]. $(La,Gd)B_3O_6:Bi$ is another borate based, UV emitting phosphor of commercial importance [32]. Cathodoluminescent phosphors $InBO_3:Tb^{3+}$ [33] and $(Y,Gd)BO_3:Tb^{3+}$ [34] are used as a green emitting phosphor in projection color TV and for PDP. In general, borates doped with suitable rare earth could be considered as good alternatives for existing phosphors as they are simple to use and can be produced at a relatively low cost.

In this report, we present a new class of stable, efficient, environmentally friendly, low cost, and easily synthesized single-phased Dy^{3+}–Eu^{3+} co-doped potassium calcium borate phosphors for the first time. These phosphors exhibits rich emission lines, covering 450–800 nm region with good white light color coordinates for various commercially available UV–violet excitation sources. The observed stable and nearly white light emission and comparatively higher life times suggest that present phosphors could be potentially applied as a white light-emitting phosphor for display and lighting.

Experimental details

The potassium calcium borate ($KCaBO_3$) phosphor co-doped with Dy^{3+}–Eu^{3+} were synthesized by solid state diffusion method [12]. Stoichiometric amounts of KCl, $CaCl_2$, and H_3BO_3 in with x.0 wt% ($x = 0$, 1–3) of Dy_2O_3 and 2.0 wt% of Eu_2O_3 were thoroughly mixed and grounded into fine powder in a mortar. Eventually this mixture was heated in air atmosphere up to 450 °C for 1 h and then to 950 °C for 21 h in a silica crucible, then was cooled to room temperature by rapid cooling. X-ray diffraction (XRD) data for all these polycrystalline samples was collected on XPERT-PRO Diffractometer with Cu Kα radiation ($\lambda = 1.54$ Å). The steady-state and time-resolved emission measurements were carried using home built setups using 410 nm diode laser as excitation source [39]. The emission light was dispersed into a monochromator (Acton SP2300) coupled to a photo multiplier tube (PMT) through appropriate lens system. For time-resolved emission, mechanical chopper (12 Hz), lock-in amplifier, and digital storage oscilloscope were employed to record the transient decay response. The excitation/emission measurements were also carried on Fluorolog fluorescence spectrophotometer (HORIBA JOBINYVON) by selecting various excitations from inbuilt xenon source.

Results and discussions

X-ray diffraction studies

Figure 1 shows the room temperature XRD patterns of undoped $KCaBO_3$ and 2 wt% Dy^{3+} co-doped $KCaBO_3:Eu^{3+}$ phosphor. The sharp and single peaks of the XRD pattern suggest the formation of single-phase polycrystalline nature and close to the reported data of similar mixed borate $LiBaBO_3$ and other doped $KCaBO_3$ phosphors [12, 35]. Essentially, the obtained $KCaBO_3$ has monoclinic crystal structure having space group of $P2_1/c$ (14), for both doped and undoped compounds [12]. Though almost all major diffraction peaks are identified with the reported data, other few low intense diffraction peaks are not resolved properly, could be due to the presence of other predominant XRD patterns. While many alkali and alkaline earth metal mixed borates have shown different crystalline phases [10–14], this study reports single-phased $KCaBO_3$. Moreover, enhanced XRD peaks (ex: (121), (210), (302)) appeared upon doping, indicating no significant changes in the host crystal structure, but facilitates better crystallinity with interstitial incorporation and possibility of heterogeneous nucleation (Table 1). However, for complete analysis and accurate

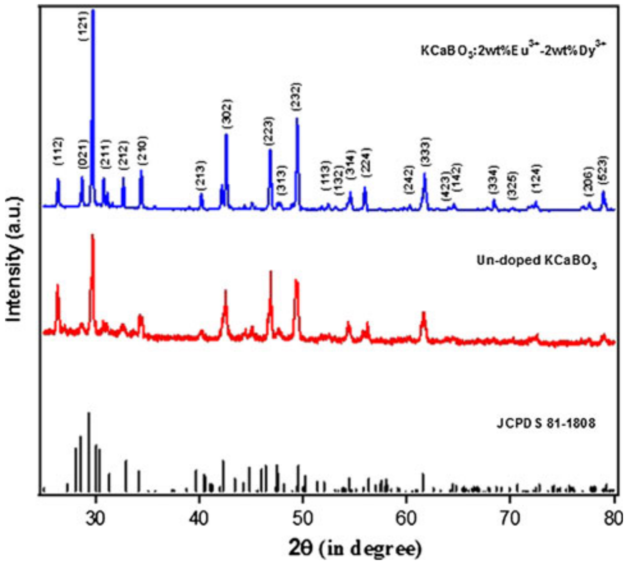

Fig. 1 Room temperature X-ray diffraction pattern of un-doped $KCaBO_3$ [12] and 2 wt% Dy^{3+} co-doped $KCaBO_3:Eu^{3+}$ compounds. Standard $LiBaBO_3$ data (JCPDS 81-1808) also given for comparison

Table 1 Lattice parameters of un-doped $KCaBO_3$ and 2 wt% Dy^{3+} co-doped $KCaBO_3$:2 wt%Eu^{3+} compounds

Compound	*a* (Å)	*b* (Å)	*c* (Å)
$KCaBO_3$ [12]	11.46	6.90	7.25
$KCaBO_3$:2 wt%Eu^{3+}–2 wt%Dy^{3+}	11.54	6.97	7.17

determination of structure, other dedicated experiments are necessary. The grain sizes estimated from the well-known Scherrer equation are in the range of 50–75 nm.

Photoluminescence (PL) studies of doped $KCaBO_3$ phosphors

PL studies under 410 nm excitation

The room temperature PL spectra of x.0 wt% ($x = 0$, 1–3) Dy^{3+} co-doped $KCaBO_3$:Eu^{3+} samples have been recorded under excitation of 410 nm, which are shown in Fig. 2a. The spectra of un-doped and individual Dy^{3+} and Eu^{3+} doped $KCaBO_3$ samples also shown for comparison. As seen the emissions at 483, 574, 658, 695, and 750 nm, are attributed to the Dy^{3+} ion energy transitions $^4F_{9/2} \rightarrow {}^6H_{J/2}$ ($J = 15$, 13, 11, 9, and 7) and emissions at 579, 594, 616, 653, and 701 nm are corresponds to Eu^{3+} transitions, $^5D_0 \rightarrow {}^7F_J$ ($J = 0$, 1, 2, 3, and 4) [36, 37]. In Dy^{3+} the emission lines yellow and blue (483 and 574 nm of $^4F_{9/2} \rightarrow {}^6H_{13/2}$ and $^6H_{15/2}$) and in Eu^{3+} red and orange (616 and 594 nm of $^5D_0 \rightarrow {}^7F_2$ and $^7F_1$) are the strongest emission lines. The hypersensitive electric dipole transition at 616 nm ($^5D_0 \rightarrow {}^7F_2$ of Eu^{3+}) was found stronger in all Dy^{3+}–Eu^{3+} co-doped samples and both red and orange emission intensities shows systematic enhancement with the increase of Dy^{3+} co-doping concentration. This could be possibly due to partial energy transfer (ET) from Dy^{3+} to Eu^{3+} ions (Fig. 2b). Though the energy of the $^4F_{9/2}$ level of Dy^{3+} (21.14×10^3 cm^{-1}) is slightly higher than that of the Eu^{3+} $^5D_0$ level (17.29×10^3 cm^{-1}), the energy transfer is possible due to the phonon-aided non-radiative relaxation from $^4F_{9/2}$ level of Dy^{3+} to the $^5D_0$ level of Eu^{3+}.

The yellow-to-blue (Y/B) ($^4F_{9/2} \rightarrow {}^6H_{13/2}/{}^4F_{9/2} \rightarrow {}^6H_{15/2}$ of Dy^{3+}) and red-to-orange (R/O) ($^5D_0 \rightarrow {}^7F_2/{}^5D_0 \rightarrow {}^7F_1$ of Eu^{3+}) emission intensity ratios will give insight into the covalent nature, and site asymmetry effects and local structure [38, 39]. Such ratios for different Dy^{3+} concentrations in co-doped in $KCaBO_3$:Eu^{3+} samples are estimated and listed in Table 2. It is observed that the both

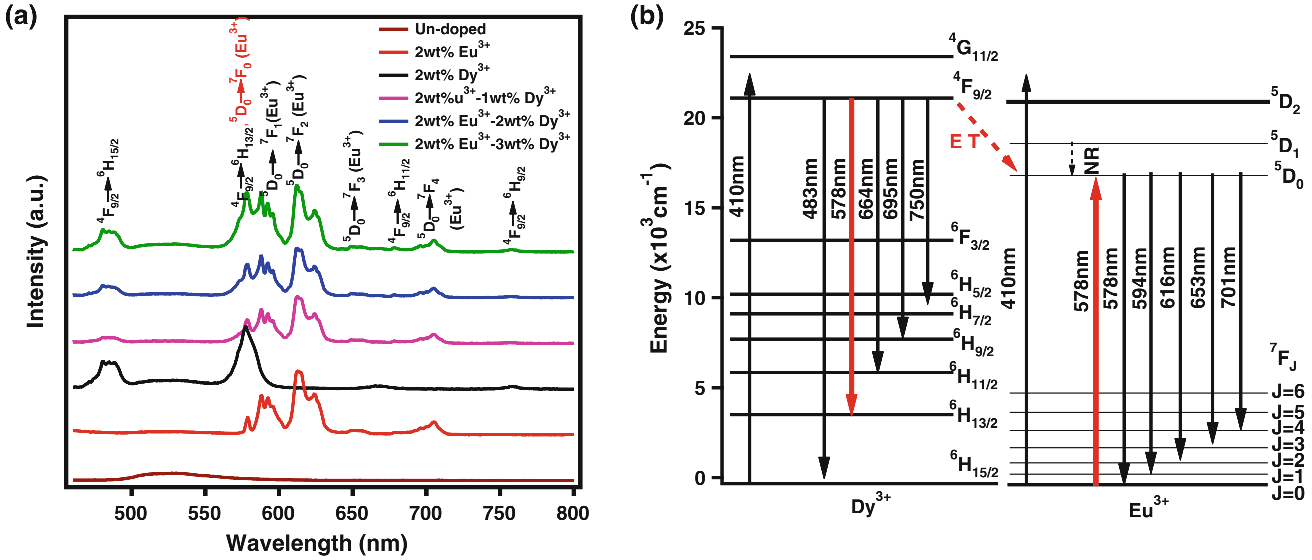

Fig. 2 **a** Room temperature PL emission spectra of un-doped $KCaBO_3$, $KCaBO_3$:2 wt%Dy^{3+}, and x.0 wt% ($x = 0$, 1, 2, 3) Dy^{3+} co-doped $KCaBO_3$:Eu^{3+} phosphors ($\lambda_{exe} = 410$ nm). **b** The schematic energy levels of Dy^{3+} and Eu^{3+} ions

Table 2 The emission lifetimes, yellow-to-blue (Y/B) and red-to-orange (R/O) integrated ratios and chromaticity coordinates of $KCaBO_3$:2 wt%Dy^{3+} and x.0 wt% ($x = 0$, 1, 2, 3) Dy^{3+} co-doped $KCaBO_3$:Eu^{3+} phosphors ($\lambda_{exc} = 410$ nm)

Doping type	Y/B ratio	R/O ratio	CIE coordinates		Emission life times (τ) (in ms)	
			X	Y	574 nm ($^4F_{9/2} \rightarrow {}^6H_{13/2}$ of Dy^{3+})	616 nm ($^5D_0 \rightarrow {}^7F_2$ of Eu^{3+})
2 wt%Dy^{3+}	2.22	–	0.355	0.449	1.83	–
2 wt%Eu^{3+}	–	1.74	0.394	0.303	–	2.49
2 wt%Eu^{3+}–1 wt%Dy^{3+}	3.97	1.36	0.477	0.411	1.86	2.32
2 wt%Eu^{3+}–2 wt%Dy^{3+}	2.81	1.16	0.431	0.403	1.80	2.22
2 wt%Eu^{3+}–3 wt%Dy^{3+}	2.63	1.35	0.423	0.415	1.69	2.16

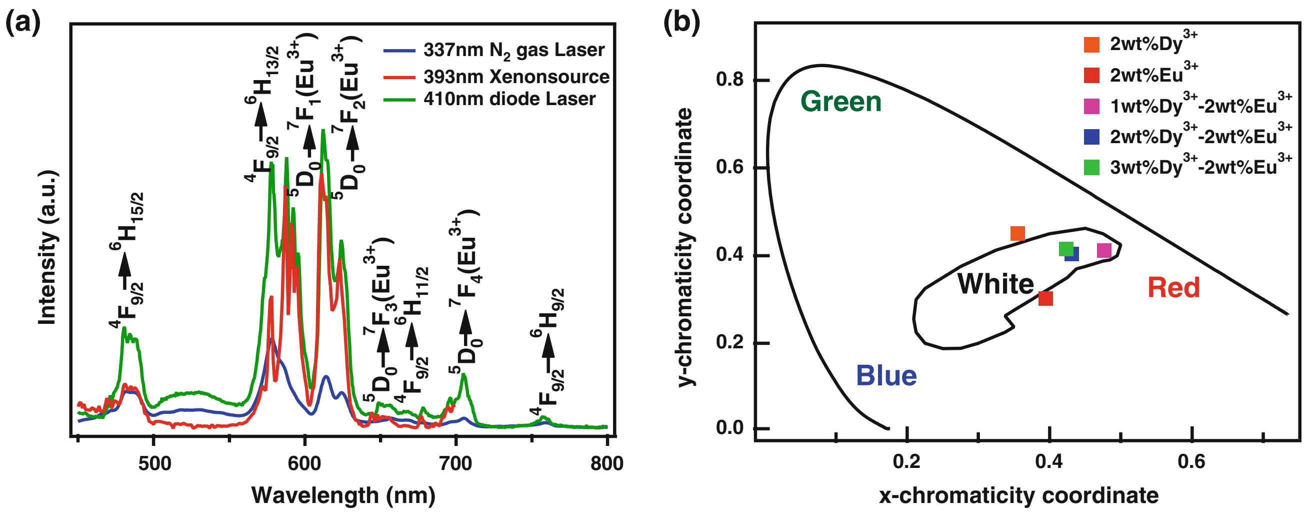

Fig. 3 Room temperature **a** PL emission spectra of 3.0 wt% of Dy^{3+} co-doped $KCaBO_3:Eu^{3+}$ phosphors ($\lambda_{exe} = 337$, 393, and 410 nm) and **b** chromaticity diagram of the emission of $KCaBO_3$:2 wt%Dy^{3+} and x.0 wt% ($x = 0, 1, 2, 3$) Dy^{3+} co-doped $KCaBO_3:Eu^{3+}$phosphors ($\lambda_{exe} = 410$ nm)

Y/B and R/O ratios are dominated by Y and R, respectively, and found to have different values for varied concentrations of Dy^{3+}. By appropriate adjustment of Dy^{3+}–Eu^{3+} ion combination, it is possible to obtain near-white emission in these doped $KCaBO_3$ phosphors (Fig. 3b).

To establish these phosphors for further applications, it is desirable to demonstrate that the emission could be obtained from various popular excitation sources of commercial interest. Figure 3a gives the emission spectra recorded at different excitation wavelengths and corresponding emission spectral features are more or less similar. A detailed discussion on the excitation spectral features will be in the following section. Further, the PL spectra of all phosphors show a less intense broad featureless emission from 500 to 550 nm, while excited with 337 and 410 nm wavelength (Figs. 2a, 3a). Such broad emission could due to the host matrix $KCaBO_3$, where the emission is due to the defects of K^+-ions lying in the interstices $KCaBO_3$ lattice [40]. However, such emission is comparatively low intense and excitation energy sensitive (Fig. 3a). In general, having wide range of excitation energies to obtain nearly white light could be one of the advantages of these studied phosphors for further white light generation applications.

PL excitation studies

To clearly demonstrate the excitation mechanism and the origin of PL in these co-doped systems, the excitation spectra of the present samples were also recorded and depicted in Fig. 4, in which the corresponding transitions are appropriately assigned and indicated. Respective excitation spectra for single doped phosphor are also included for comparison. These co-doped phosphors exhibit rich excitation lines, characteristic of individual rare earths, and the spectral features are more or less similar. While the PL

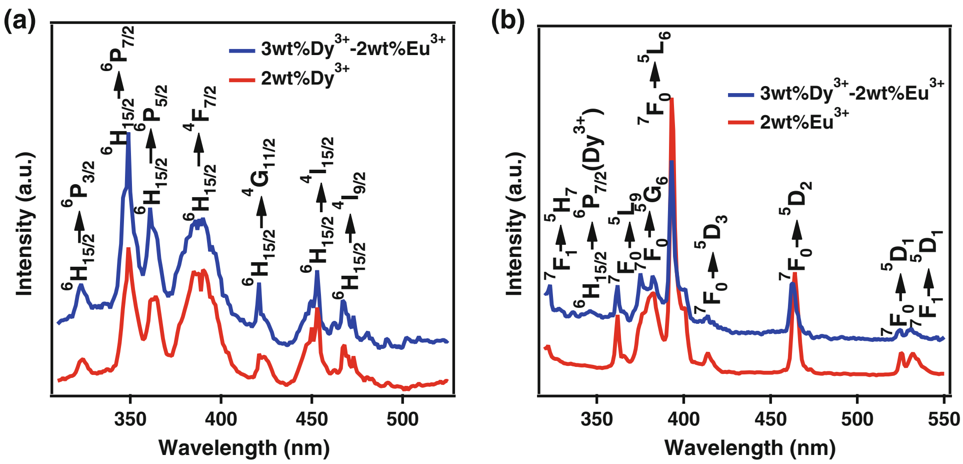

Fig. 4 Room temperature excitation spectra of **a** $KCaBO_3$:2 wt%Dy^{3+} and 3 wt% Dy^{3+} co-doped $KCaBO_3:Eu^{3+}$ phosphors monitored at 574 nm ($^4F_{9/2} \rightarrow {}^6H_{13/2}$ of Dy^{3+}) emission and **b** $KCaBO_3$:2 wt% Eu^{3+} and 3 wt% Dy^{3+} co-doped $KCaBO_3:Eu^{3+}$ phosphors monitored at 616 nm ($^5D_0 \rightarrow {}^7F_2$ of Eu^{3+}) emission

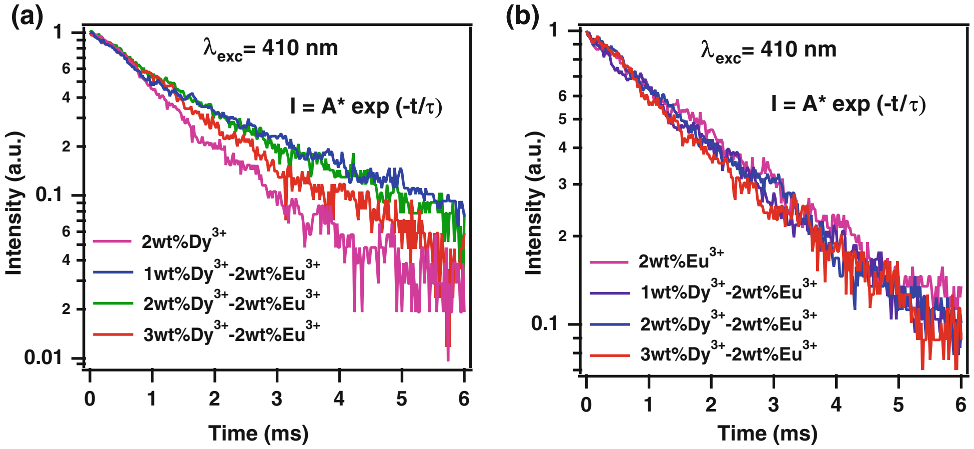

Fig. 5 The decay curves of **a** 574 nm ($^4F_{9/2} \rightarrow {}^6H_{13/2}$ of Dy^{3+}) emission and **b** 616 nm emission ($^5D_0 \rightarrow {}^7F_2$ of Eu^{3+}) in $KCaBO_3$:2 wt%Dy^{3+} and x.0 wt% (x = 0, 1, 2, 3) Dy^{3+} co-doped $KCaBO_3$:Eu^{3+} phosphors (λ_{exe} = 410 nm)

excitation (Fig. 4b) spectra corresponding to the PL at 616 nm emission of Eu^{3+} ions show typical transitions from $^7F_0$ and $^7F_1$ to the various excited states of Eu^{3+}, the co-doped system shows additional excitation band at about 350 nm correspond to solely Dy^{3+} ion, $^6H_{15/2} \rightarrow {}^6P_{3/2}$ excitation transition. This is an indication of possible inter-ion energy transfer from Eu^{3+} to Dy^{3+} ions. In general, the Eu^{3+} emission in some of the oxide based phosphors is sensitive to the site selectivity of doped rare earth ions [37]. The present results of invariant emission upon various excitations (Fig. 3a) indicating that the site selectivity of excitation is not prominent suggesting that the rare earth ions are situated in the matrix predominantly in a single site, i.e., the charge compensated position of Ca^{2+}. In general, the excitation spectra of these phosphors have rich excitation lines (300–600 nm), enabling the excitation from most of the available UV/blue excitation sources such as InGaN based LED chips for potential application as white light LEDs.

PL life time studies

The PL intensity decay curves for the yellow (574 nm, $^4F_{9/2} \rightarrow {}^6H_{13/2}$ of Dy^{3+}) and orange (616 nm, $^5D_0 \rightarrow {}^7F_2$ of Eu^{3+}) emissions in co-doped $KCaBO_3$ phosphors are recorded using 410 nm laser and the setup explained in the experimental section. The experimentally obtained PL intensity decay curves for individual emissions of Dy^{3+} and Eu^{3+} components are presented in Fig. 5a and b, respectively. All the experimental emission decay curves were found to be predominately single exponential and the decay curves can be fitted into the general exponential equation, $I = A \cdot \exp(-t/\tau)$, where A is the integrated area and τ is the PL life time. The obtained life time values from the fits are given in Table 2. However, the decay curves show slightly double exponential nature with another shorter life time of about 0.9 ms with less than 10% component. Such double exponential nature could be due to the existence cross-relation mechanism between co-doped rare earth ions, supporting our earlier discussion. However, the predominant single exponential behavior indicating the homogeneous distribution of doped ions inside the host matrix. Further, it is evident that the life times of Dy^{3+} emission (at 574 nm) mixed doped phosphors are slightly shorter than the values obtained for singly doped sample and similar is the trend for 616 nm (Eu^{3+} emission) as well. In general, the lifetimes of 616 nm emission decreases gradually with the increased Dy^{3+} concentration from 1.0 to 3.0 wt%, which is a further supporting evidence of the inter-ion energy transfer. Further, the present life time values are comparatively higher to that of other phosphors reported earlier [41].

Chromaticity diagram

In general, color of any phosphor material is represented by means of color coordinates. Therefore, the CIE chromaticity coordinates of the light emission from these co-doped $KCaBO_3$ phosphors excited at 410 nm are as shown in Fig. 3b and the coordinates are listed in Table 2. In our present study appropriate adjustment of Dy/Eu doping concentrations were tested to obtain white light emission. As seen that the typical white light is achieved for all co-doped systems where 3 wt% Dy^{3+} co-doped $KCaBO_3$:Eu^{3+} exhibits pure white light with CIE coordinates of (X = 0.42, Y = 0.41), while the individual doped Dy^{3+} and Eu^{3+} phosphors fall in green and red regions, respectively. This adjustability of luminescence color can also broaden the application areas.

Conclusions

Single-phase monoclinic $KCaBO_3$:2 wt%Dy^{3+} and x.0 wt% (x = 0, 1, 2, 3) Dy^{3+} co-doped $KCaBO_3$:Eu^{3+} samples were prepared by solid sate diffusion technique at

950 °C and their luminescence have been studied and discussed for the first time. These phosphors can excited by UV and blue lights which are in agreement with UVLED and blue LED chips. Most importantly Dy^{3+} co-doped $KCaBO_3:Eu^{3+}$ samples emit white light under blue excitation. While $KCaBO_3$:2 wt%Dy^{3+} and $KCaBO_3$:2 wt%Eu^{3+} samples exhibit strong greenish yellow (574 nm) and red (612 nm) emissions under 410 nm excitations. Based on these emission results we propose that the newly prepared $KCaBO_3$:2 wt%Dy^{3+}, $KCaBO_3$:2 wt%Eu^{3+}, and Dy^{3+} co-doped $KCaBO_3:Eu^{3+}$ samples are very promising phosphors for red, greenish yellow and white LEDs, respectively.

References

1. Green WH, Le KP, Grey J, Au TT, Sailor MJ (1997) Science 276:1826
2. Wang B, Sun L, Ju H (2010) Sol State Commun 150:1460
3. Li P, Wang Z, Yang Z, Guo Q, Li X (2010) J Lumin 130:222
4. Kuo CH, Sheu JK, Chang SJ, Su YK, Wu LW, Tsai JM, Liu CH, Wu RK (2003) Jpn J Appl Phys 42:2284
5. Kim JS, Jeon PE, Choi JC, Park HL, Mho SI, Kim GC (2004) Appl Phys Lett 84:2931
6. Kim JS, Kang JY, Jeon PE, Chol JC, Park HL, Kim TW (2004) Jpn J Appl Phys 43:989
7. Kim JS, Kang JY, Jeon PE, Park YH, Choi JC, Park HL, Kim GC, Kim TW (2004) Appl Phys Lett 85:3696
8. Rui Z, Xiang W (2011) J Alloys Compd 509:1197
9. Wu ZC, Liu J, Hou WG, Xu J, Gon ML (2010) J Alloys Compd 498:139
10. Li P, Wang Z, Yang Z, Guo Q (2010) J Rare Earths 28:523
11. Li P, Wang Z, Yang Z, Guo Q, Fu G, Li XZ, Xu YP (2009) Mater Res Bull 44:2068
12. Das S, Amarnath Reddy A, Vijaya Prakash G (2011) Chem Phys Lett 504:206
13. Wu L, Zhang Y, Kong YF, Sun TQ, Xu JJ, Chen XL (2007) Inorg Chem 46:5207
14. Wu L, Chen XL, Li H, He M, Xu YP, Li XZ (2005) Inorg Chem 44:6409
15. Guoqing Z, Jun X, Xingda C, Heyu Z, Siting W, Ke X, Peizhen D, Fuxi G (1998) J Cryst Growth 191:517
16. Ogorodnikov IN, Kuznetsov AY, Kruzhalov AV, Maslov VA (1995) Rad Meas 24:423
17. Keszler DA, Tu JM (1995) Mater Res Bull 30:209
18. Hu ZG, Higashiyama T, Yoshimura M, Mori Y, Sasaki T (2000) J Cryst Growth 212:368
19. Aka G, Mougel F, Augé F, Harari AK, Vivien D, Bénitez JM, Salin F, Pelenc D, Balembois F, Georges P, Brun A, Nain NL, Jacquet M (2000) J Alloy Comp 303–304:401
20. Guifang L, Quanxi C, Zhimin L, Yunxia H (2008) J Rare Earths 26:792
21. Petrov V, Rotermund F, Noack F, Komatsu R, Sugawara T, Uda S (1998) J Appl Phys 84:5887
22. Kutomi Y, Khrmta MH, Durrani SA (1995) Rad Meas 24:407
23. Furetta C, Kitis G, Weng PS, Chu TC (1999) Nucl Instrum Methods A 420:441
24. Dhoble SJ, Moharil SV (1999) Nucl Instrum Methods B 160:274
25. Knitel MJ, Hommels B, Dorenbos P, van Eijk CWE, Berezovskaya I, Dotsenko V (2000) Nucl Instrum Methods A 449:595
26. Holsa J, Leskela M (1991) J Lumin 48–49:497
27. Knitel MJ, Dorenbos P, Andriessen J, van Eijk CWE, Berezovskaya I, Dotsenko V (1998) Rad Meas 29:327
28. Srivastava AM, Doughty DA, Beers WW (1996) J Electrochem Soc 143:4113
29. Smets BMJ (1991) Mater Chem Phys 16:283
30. Saakes M, Leskela M, Blasse G (1984) Mater Res Bull 19:151
31. Machid K, Adachi G, Shiokawa J (1979) J Lumin 21:101
32. Blasse G, Grabmaier BC (1994) Luminescent materials. Springer-Verlag, Berlin
33. Chaminade JP, Garcia A, Pouchard M, Fouassier C, Jacquier B, Gallix DP, Mestres LG (1990) J Cryst Growth 99:799
34. Kwon IE, Yu BY, Bae H, Hwang YJ, Kwon TW, Kim CH, Pyun CH, Kim SJ (2000) J Lumin 87:1039
35. Schlaeger M, Hoppe MRZ (1997) Anorg Allg Chem 619:976
36. Yang HC, Li CY, He H, Tao Y, Xu JH, Su Q (2006) J Lumin 118:61
37. Yanlin H, Seo HJ (2011) J Electrochem Soc 158:215
38. Vijaya Prakash G, Jagannathan R (1999) Spectrochim Acta A 55:1799
39. Amarnath Reddy A, Chandra Sekhar M, Pradeesh K, Surendra Babu S, Vijaya Prakash G (2011) J Mater Sci 46:2018. doi: 10.1007/s10853-010-4851-3
40. Bhaskar R, Lakshmanan AR, Sundarrajan M, Ravishankar T, Jose MT, Lakshminarayan N (2009) Indian J Pure Appl Phys 47:772
41. Qin C, Huang Y, Chen G, Shi L, Qiao X, Gan J, Seo HJ (2009) Mater Lett 63:1162